Plant, Cell and Environment (2004) **27**, 509–519

Scaling phloem transport: information transmission

M. V. THOMPSON* & N. M. HOLBROOK

Department of Organismic and Evolutionary Biology, Harvard University, Biological Laboratories, 16 Divinity Avenue, Cambridge, Massachusetts, USA

ABSTRACT

Sieve tubes are primarily responsible for the movement of solutes over long distances, but they also conduct information about the osmotic state of the system. Using a previously developed dimensionless model of phloem transport, the mechanism behind the sieve tube's capacity to rapidly transmit pressure/concentration waves in response to local changes in either membrane solute exchange or the magnitude and axial gradient of apoplastic water potential is demonstrated. These wave fronts can move several orders of magnitude faster than the solution itself when the sieve tube's axial pressure drop is relatively small. Unlike the axial concentration drop, the axial pressure drop at steady state is independent of the apoplastic water potential gradient. As such, the regulation of whole-sieve tube turgor could play a vital role in controlling membrane solute exchange throughout the translocation pathway, making turgor a reliable source of information for communicating change in system state.

Key-words: dimensionless model; sieve tube; wave propagation; impulse response; osmoregulatory flow.

INTRODUCTION

An unresolved issue in the study of phloem translocation is the speed with which a change in sieve tube state is transmitted along its length. Intuitively, the transmission of pressure change ought to be set by the membrane and elastic properties of the sieve tube (Kallarackal & Milburn 1985), while the transmission of a change in concentration would be set by the time required for solution to move the length of the sieve tube. However, direct observation has shown that pressure and concentration fronts propagate much faster than the solution itself, sometimes by more than an order of magnitude (Mason & Maskell 1928a, b; Huber, Schmidt & Jahnel 1937; Zimmermann 1969; Moorby, Troughton & Currie 1974; Lee 1981).

Zimmermann (1969) argued that 'pressure/concentration' waves (Ferrier, Tyree & Christy 1975; Ferrier 1976) are the combined result of local osmotic responses to changes in apoplastic water potential, and thus the result of pressure propagation in the xylem rather than in the phloem. In contrast, Ferrier *et al*. (1975), using a now standard physicochemical and fluid mechanical modelling approach to phloem translocation, showed that both changes in the apoplastic water potential gradient and changes in solute loading would have the same effect on pressure/concentration wave propagation.

The most plausible explanation for rapid concentration wave propagation requires that the water potentials of the sieve sap and apoplast be tightly coupled. Pressure waves develop and propagate due to a local change or imbalance in water potential. These waves drive membrane water flux elsewhere in the sieve tube, either diluting or concentrating the solution until the sieve sap again comes into water potential equilibrium with the apoplast. If the pressure waves propagate quickly, so will the concentration waves, as long as the sieve sap can quickly return to water potential equilibrium, which, in turn, depends on the local elastic and membrane properties of the sieve tube (Dainty 1976; Kallarackal & Milburn 1985).

An analytical expression of the time scales involved in wave propagation was presented by Ferrier (1976), but the assumptions involved limit its usefulness. Here, using the model of Thompson & Holbrook (2003b), we show that the rate of transmission of pressure and concentration 'information' depends on a single dimensionless scale, $\hat{F}$, also called the phloem transport scale, which corresponds to the ratio of the osmotic pressure of the solution to the magnitude of the axial pressure drop. The phloem transport scale has great diagnostic value as a comparative tool across a variety of phloem transport scenarios, and here serves as an index of the relative efficiency of the transport phloem for information transmission in response to change.

METHODS

This work outlines factors critical to pressure/concentration wave propagation, as well as a set of analytical and numerical methods that can be used to estimate its speed. The numerical methods employed here are the same as those used by Thompson & Holbrook (2003b).

Governing equations

Thompson & Holbrook (2003b) showed that for a probable and extensive set of phloem translocation scenarios, sap in

Correspondence: Matthew V. Thompson. Fax: +1 859 2577125; e-mail: matthew.thompson@uky.edu

**Current address: Agronomy Department, University of Kentucky, Plant Sciences Building, 1405 Veterans Drive, Lexington, Kentucky, 40546, USA.*

the transport phloem (Fig. 1) is in water potential equilibrium with the apoplast. This is a commonly made assumption (Fisher 1978; Minchin, Thorpe & Farrar 1993; Patrick *et al*. 2001), but previously with little justification.

In water potential equilibrium, the relevant transport equations greatly simplify, pinning sieve tube dynamics solely on the value of a dimensionless group denoted by $\hat{F}$ (also called the 'phloem transport scale', see Thompson & Holbrook 2003b). Mathematically, $\hat{F}$ is the ratio of the sieve sap's osmotic pressure, Ψ_π, to the flow rate- and geometry-dependent pressure drop, Π, attendant along the translocation path:

$$\hat{F} = \frac{\Psi_\pi}{\Pi} \tag{1}$$

(In the plant physiology literature, the symbol Π commonly refers to osmotic pressure, but here, to maintain parallelism between the variable and scale symbols, it refers to the axial hydrostatic pressure drop; hence, p: Π, v: U, t: τ.) Both Ψ_π and Π are in units of pressure, so $\hat{F}$ is dimensionless. Conceptually, $\hat{F}$ reflects whether a local perturbation in sieve tube state is more likely to propagate axially ($\hat{F} > 1$) or to accumulate locally ($\hat{F} < 1$). This is intuitively obvious from observation of dimensionless solute profiles at different values of $\hat{F}$ (Fig. 1), where a much larger solute concentration gradient is attendant at low $\hat{F}$ than at high $\hat{F}$, indicating facile axial propagation at large $\hat{F}$ (Fig. 1).

When in water potential equilibrium, pressure and solute concentration locally co-vary in response to perturbation. An increase in local solute concentration will lead to an influx of water that will raise the pressure until the balance is restored. Furthermore, a propagating pressure wave will be accompanied by a concentration wave as the increased pressure drives water out of the sieve tube, concentrating the solute already present. The propagation of these waves can be thought of as 'information' transmission, both as a whole sieve tube signal of disturbance (i.e. a change in apoplastic water potential, aphid probing, mechanical damage, sun flecks in a complex canopy) and as a feedback signal for photosynthesis and allocation of solutes.

Some analysis is required to understand how this 'information' propagation works. If, along the transport phloem, net loading of solutes is low and water potential equilibrium is maintained, then the phloem transport equations of Thompson & Holbrook (2003b) can be simplified to yield the following dimensionless partial differential equation (see Tables 1 and 2 for symbol definitions):

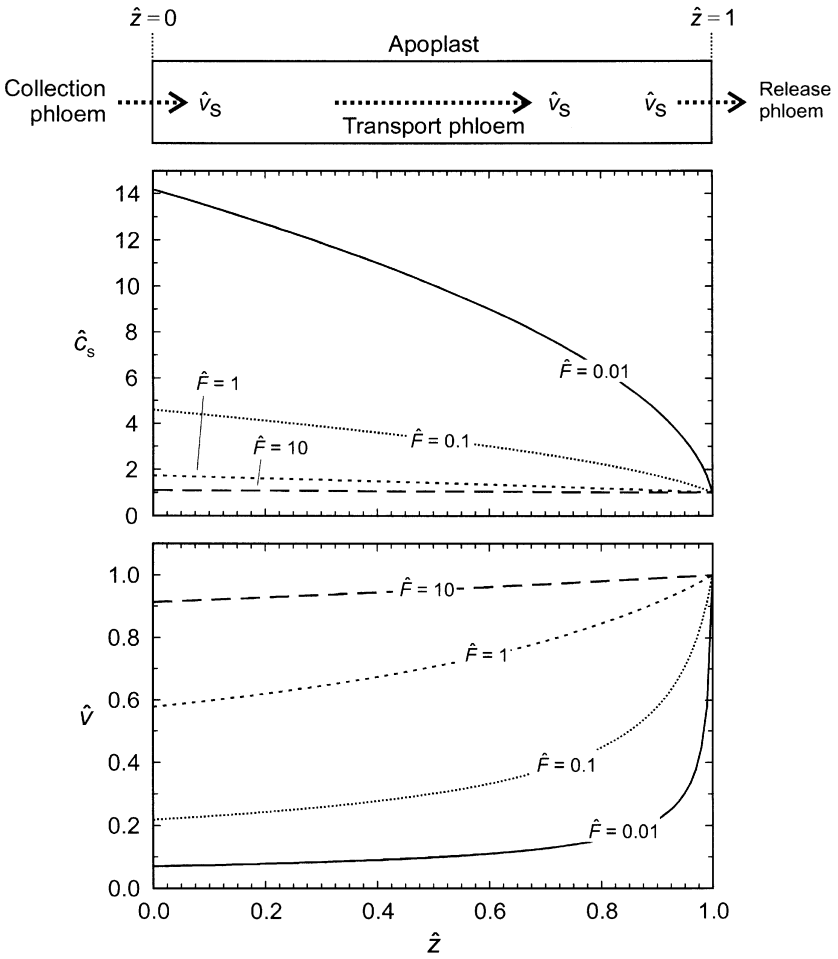

Figure 1. Steady-state behaviour of the transport phloem. Upper panel: the transport phloem in water potential equilibrium is modelled by a single dimensionless differential equation with solute flux boundary conditions defined at the 'borders' between the transport phloem and the collection and release phloem (at $\hat{z} = 0, 1$). Membrane solute flux in the transport phloem is assumed negligible. Lower panels: steady-state dimensionless concentration ($\hat{c}_s$) and velocity ($\hat{v}$) profiles of sieve tubes in water potential equilibrium, and at $\hat{\psi}_o$ ($\hat{z}$) = 0, as a function of $\hat{F}$. At $\hat{F} = 10$ and above, the concentration drop becomes negligible. At $\hat{F} = 1$, the concentration drop is of the same order of magnitude as the mean concentration in the sieve tube. At $\hat{F} < 1$, the concentration drop becomes very large. The velocity profile at steady-state is simply $1/\hat{c}_s$ since the solute flux density $\hat{v}_s$ is unity for all $\hat{z}$ (i.e. mass conservation requires that $\hat{v}_s$ be the same everywhere). $\hat{v}$ is an increasing function of $\hat{z}$ due to the axial drop in pressure and constant influx of water along the sieve tube's length.

Table 1. Parameter and scale definitions. All symbols with carets refer to dimensionless parameters or variables

Parameter or scale	Units	Definition
A_0, A_1	–	Amplitude of normalized concentration variation at $\hat{z} = 0$ and 1, respectively,
$\hat{d}$	–	Dimensionless amplitude of loading function (Eqn 8)
$\hat{f}$	–	Dimensionless frequency of loading function (Eqn 8)
I	mol m^{-2} s^{-1}	Solute transport scale (steady-state axial solute transport rate)
k	m^2	Sieve tube specific conductivity
L	m	Length scale (sieve tube length)
L_p	m s^{-1} MPa^{-1}	Sieve tube membrane permeability
r	m	Sieve tube radius
$\Re$	MPa m^3 mol^{-1} K^{-1}	Universal gas constant (8.3143×10^{-6})
T	K	Temperature
U	m s^{-1}	Solution flux density scale (solution velocity, $U = I/\Phi$)
$\hat{\alpha}$	–	Loading function (Eqn 8), $\hat{\alpha} = \hat{\alpha}\ (\hat{t})$
ε	MPa	Volumetric elastic modulus, or drained pore modulus, of the sieve tube (see Thompson & Holbrook 2003a)
μ	MPa s	Viscosity scale (sap dynamic viscosity), $\mu = \mu(\Phi, T)$
Π	MPa	Pressure scale (approximate turgor pressure drop along the sieve tube's length), $\Pi = \mu LU/k$
τ	s	Time scale (length scale divided by velocity scale, or $\tau = L/U$)
Φ	mol m^{-3}	Concentration scale (set-point unloading zone concentration)
Ψ_π	MPa	Sieve sap osmotic pressure, $\Psi_p = \Re T\Phi$
$\hat{F}$	–	Phloem transport scale (ratio of sap osmotic strength to pressure scale), $\hat{F} = \Psi_\pi/\Pi$

$$\frac{\partial}{\partial \hat{t}}\hat{c}_s = \frac{\partial}{\partial \hat{z}}\left(\hat{c}_s \frac{\partial}{\partial \hat{z}}\left[\hat{\psi}_o + \hat{F}\hat{c}_s\right]\right) \quad (2)$$

whose dynamics depend solely on the value of $\hat{F}$. The left side of Eqn 2 reflects the temporal change in solute concentration, the quantity in the parentheses is the axial solute flux, and the quantity in square brackets is same as the hydrostatic pressure of the sap (since $\hat{p} = \hat{\psi}_o + \hat{F}\hat{c}_s$, i.e. water potential equilibrium). The first boundary condition on Eqn 2 (Fig. 1) is the solute flux density [$\hat{v}_s$, where $\hat{v}_s = \hat{c}_s \partial\left(\hat{\psi}_o + \hat{F}\hat{c}_s\right)/\partial \hat{z}$ for all $\hat{z}$] from the collection phloem to the transport phloem:

$$\hat{v}_s = \hat{\alpha}(\hat{t}) \text{ at } \hat{z} = 0 \quad (3)$$

where $\hat{\alpha}$ is an arbitrary function of time. The other boundary condition is the solute flux density from the transport to the release phloem, and is a linear function of concentration:

$$\hat{v}_s = \hat{c}_s \text{ at } \hat{z} = 1 \quad (4)$$

At steady-state, it can be shown that $\partial \hat{v}_s/\partial \hat{z} = 0$ for all $\hat{z}$, allowing the following analytical solution of Eqn 2 for $\hat{\psi}_o = 0$ (see Fig. 1):

$$\hat{c}_s\ (\hat{z}) = \left[\frac{2}{\hat{F}}(1-\hat{z}) + 1\right]^{1/2} \quad (5)$$

As long as axial efflux is proportional to concentration, per Eqn 4, the unloading response to system perturbation will be inherently exponential. Other unloading schemes are possible (see Goeschl & Magnuson 1986; Minchin *et al.* 1993), but since we are more concerned with wave propa-

Table 2. Variable and dimensionless variable definitions

Variable	Units	Definition	Dimensionless variable
c_s	mol m^{-3}	Solute concentration	$\hat{c}_s = c_s/\Phi$
p	MPa	Turgor (pressure)	$\hat{p} = p/\Pi$
t	s	Time	$\hat{t} = t/\tau$
v	m s^{-1}	Solution flux density	$\hat{v} = v/U$
v_s	mol m^{-2} s^{-1}	Solute flux density	$\hat{v}_s = v_s/I$
z	m	Axial position	$\hat{z} = z/L$
ψ_o	MPa	Apoplastic water potential	$\hat{\psi}_o = \psi_o/\Pi$
ψ_π	MPa	Sap osmotic potential ($\psi_\pi = -\Re T c_s$)	$\hat{\psi}_\pi = \psi_\pi/\Pi$
τ_p	s	Wave propagation time	$\hat{\tau}_p = \tau_p/\tau$
τ_t	s	Transit time (Eqn 7), Thompson & Holbrook (2003b) use $\bar{\tau}$	$\hat{\tau}_t = \tau_t/\tau$
τ_e	s	Elastic response time (see Eqn 11)	$\hat{\tau}_\varepsilon = \tau_e/\tau$

gation in the transport phloem than with the nature of solute unloading, we use the simplest unloading condition to ease interpretation. We confine the behaviour of Eqn 2 to variation in the loading boundary condition (Eqn 3), apoplastic water potential $\hat{\psi}_o$ (an exogenous forcing function), and $\hat{F}$, which when expanded is given by:

$$\hat{F} = \frac{\Psi_\pi}{\Pi} = \Re T \Phi \frac{k}{\mu L U} \tag{6}$$

Equations 2, 3 and 4 are numerically solved with Eqn 5 as an initial condition using a finite difference advection scheme with a total-variation diminishing method to reduce solute smearing at sharp solute boundaries (Thompson & Holbrook 2003a). The simulation is 100% mass conservative, and is available in MATLAB version 6.5 code from the authors.

Transport time scales

We employ several time scales (Table 2), the relative magnitudes of which shed insight into the processes that limit 'information' transmission. The first is the time scale of the system (τ), which is used to make all other temporal scales dimensionless (i.e. $\hat{t} = t/\tau$, Table 1). One unit of $\hat{t}$ corresponds to the dimensionless time required for solute to move the length of the sieve tube at the velocity of the sieve sap at $\hat{z} = 1$. However, because solution velocity in a sieve tube with no net radial solute flux is nowhere as high as it is at $\hat{z} = 1$ (see Fig. 1), τ is an underestimate of transit time. Instead, dimensionless transit time $\hat{\tau}_t$ is used, where $\hat{\tau}_t = \tau_t/t$ (Thompson & Holbrook 2003b, use the symbol $\bar{\tau}$ to denote transit time), and is given by the integral from $\hat{z} = 0$ to 1 of Eqn 5:

$$\hat{\tau}_t = \frac{\hat{F}}{3}\left[\left(\frac{2}{\hat{F}} + 1\right)^{3/2} - 1\right] \tag{7}$$

which is precisely valid only for $\partial\hat{\psi}_o/\partial\hat{z} = 0$, but a good approximation for $\partial\hat{\psi}_o/\partial\hat{z} \neq 0$.

Wave propagation time (τ_p) is the time required for a pressure/concentration wave to travel the length of the sieve tube. The dimensionless wave propagation time ($\hat{\tau}_p = \tau_p/t$) can be calculated numerically by running the numerical model to quasi-steady state with the following sinusoidally varying loading function:

$$\hat{\alpha} = 1 + \frac{\hat{d}}{2}\sin\left(2\pi\hat{f}\hat{t}\right) \tag{8}$$

where $\hat{f}$ is dimensionless frequency (or number of oscillations per dimensionless time), and $\hat{d}$ is dimensionless amplitude. The rate of wave propagation is then measured directly from the numerical results. Note that $\hat{d}$ must be small (< 0.01) to avoid a shift in the value of $\hat{F}$ during the simulation. The attenuation in the amplitude of the propagating wave is given by the ratio of the normalized amplitude of the wave at $\hat{z} = 1$ to the normalized amplitude of the wave at $\hat{z} = 0$, or A_1/A_0.

The dimensionless propagation time $\hat{\tau}_p$ can also be estimated analytically. When $\hat{\psi}_o$ is set equal to zero, Eqn 2 becomes a non-linear parabolic partial differential equation similar to the classical diffusion equation (although no diffusion is actually involved):

$$\frac{\partial}{\partial\hat{t}}\hat{c}_s = \frac{\partial}{\partial\hat{z}}\left(\hat{F}\hat{c}_s\frac{\partial}{\partial\hat{z}}\hat{c}_s\right) \tag{9}$$

The propagation time, $\hat{\tau}_p$, can be derived from the transport coefficient of Eqn 9 ($D = \hat{F}\hat{c}_s$) as the mean Gaussian spreading time (Berg 1993) required for a pulse of solute to travel a distance $\Delta\hat{z} = 1$:

$$\hat{\tau}_p \approx \frac{(\Delta\hat{z})^2}{2\hat{F}\hat{c}_s} = \frac{1}{2\hat{F}\hat{c}_s}\bigg|_{\Delta\hat{z}=1} \tag{10}$$

While it is possible to generally apply Eqn 10 for qualitative predictions of wave propagation time, it is only *precisely* valid when $\hat{F} > 1$ and when applied to low-frequency and low-amplitude loading functions (i.e. $\hat{f}$ and $\hat{d}$ are small, Eqn 8).

Because dimensionless concentration, axial pressure drop, time, and distance are all scaled to be of order unity, the critical value of $\hat{F}$ is also near unity. At $\hat{F} > 1$, $\hat{\tau}_p$ falls below unity; at $\hat{F} < 1$, $\hat{\tau}_p$ becomes greater than unity (that is, greater than the time scale of the system). This becomes conceptually tractable if we think of $\hat{F}$ as indicating the relative tendency of pressure and concentration impulses to propagate axially rather than accumulate in place. In sieve tubes of low $\hat{F}$, local changes in pressure and concentration will accumulate rather than propagate, wheres in sieve tubes of high $\hat{F}$, changes will propagate rather than accumulate.

Following perturbation, water potential equilibrium is not precisely maintained. The elastic response time τ_ε is the e-folding time (that is, the time required to come within 1/e of steady-state) for changes in cell volume following small perturbations in either internal osmotic potential or external water potential (Dainty 1976), given here for a right cylinder of radius r with infinite axial rigidity:

$$\hat{\tau}_\varepsilon = \frac{r}{2L_p(\varepsilon + \Psi_\pi)} \tag{11}$$

where L_p is membrane permeability (around 5.0×10^{-8} m s^{-1} MPa^{-1}, see Thompson & Holbrook 2003b), ε is the drained pore modulus of the sieve tube (between 5 and 18 MPa, see Thompson & Holbrook 2003b), Ψ_π is the sap osmotic pressure (approximately 2.0 MPa), and $2/r$ is the surface area : volume ratio of a right cylinder. For a sieve tube of $r = 40$ μm, $\varepsilon = 5$ MPa, and $\Psi_\pi = 2.0$ MPa, τ_ε would equal 57 s. In this case, the local recovery of water potential equilibrium will occur at a time scale of about 57 s. However, despite the presence of local disturbance, pressure will continue to propagate at the rate prescribed by $\hat{\tau}_p$, leaving the concentration wave to catch up. Thus, the minimum possible time scale for transmission of pressure 'information' would be no smaller than 57 s, regardless of $\hat{F}$. By

contrast, for a sieve tube of $r = 3\ \mu$m, $\varepsilon = 18$ MPa, and $\Psi_\pi = 2.0$ MPa, τ_ε would be only 1.5 s.

Change in apoplastic water potential

Axial solute flux will transiently vary following changes in the gradient of apoplastic water potential, a response that will depend not only on the change in $\hat{\psi}_o$, but also on the value of $\hat{F}$. To compare across different values of $\hat{F}$, however, it is necessary to properly scale the imposed gradient in $\hat{\psi}_o$, which can be done by casting the change in $\partial\hat{\psi}_o/\partial\hat{z}$ relative to $\partial\hat{p}/\partial\hat{z}$, which is scaled to be approximately equal to unity, at all $\hat{F}$. The same increase in $\partial\hat{\psi}_o/\partial\hat{z}$, irrespective of $\hat{F}$, will always cause the same initial and instantaneous reduction in dimensionless axial flow rate. Here, we run the simulation to steady-state with $\hat{\psi}_o = 0$ for all $\hat{z}$ and $\hat{t}$, and then change $\hat{\psi}_o$ to:

$$\hat{\psi}_o = 0.01(\hat{z} - 1) \tag{12}$$

That is, $\hat{\psi}_o = 0$ at $\hat{z} = 1$, with a gradient of $\partial\hat{\psi}_o/\partial\hat{z} = 0.01$ at all $\hat{z}$. This imposes an instantaneous 1% reduction in solution flux density ($\hat{v}$), and causes $\hat{c}_s$ to build until the axial solute flux density ($\hat{v}_s$) is again constant for all $\hat{z}$.

Comparison to data: change in length scale

These dimensionless simulations and analyses can be compared against real situations by multiplying, or 're-scaling', each dimensionless variable by its corresponding scale as a function of sieve tube length. We focused on sieve tubes of two species for which measured sieve tube geometry data are available: *Robinia pseudoacacia*, a leguminous tree, and *Ricinus communis*, a euphorb crop plant with high axial conductivity (Thompson & Holbrook 2003b): for *R. pseudoacacia*, $T = 20$ °C, $\Phi = 463.23$ mol m^{-3} (or 15% w/w, corresponding to $\mu = 1.59 \times 10^{-9}$ MPa s), $r = 10\ \mu$m, $k = 4.0 \times 10^{-12}$ m^2, and $U = 1.4 \times 10^{-4}$ m s^{-1}; and for *R. communis*, $T = 20$ °C, $\Phi = 450$ mol m^{-3} (corresponding to $\mu = 1.57 \times 10^{-9}$ MPa s), $r = 15\ \mu$m, $k = 24.7 \times 10^{-12}$ m^2, and $U = 4.0 \times 10^{-4}$ m s^{-1}. These scales and parameters were kept constant for both plants, while only length was allowed to vary. We assume that if the loading rate varies diurnally (following Eqn 8), then the frequency is once per 24 h, or, in dimensionless terms, $\hat{f} = \tau/(24\text{ h}) = L/(24\text{ h} \cdot U)$.

RESULTS

The relationship between $\hat{F}$ and wave propagation can be shown by applying a pulse of solute to the loading end of the sieve tube and tracking the perturbation in solute efflux (Fig. 2). When $\hat{F}$ exceeds unity, the solute efflux response is exponential with essentially no delay between when the solute impulse is applied and when the effect of that impulse is first observed at $\hat{z} = 1$. When $\hat{F}$ is less than or equal to unity, there is a delay while pressure and concentration build and eventually traverse the length of the sieve tube.

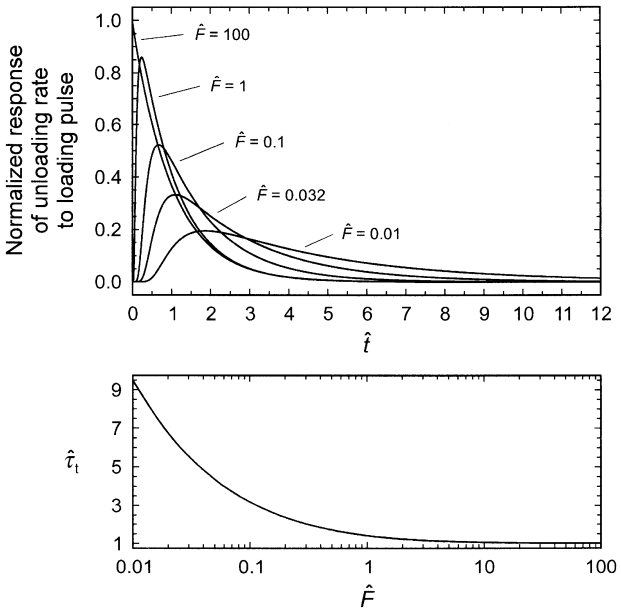

Figure 2. Transport of information and material as a function of $\hat{F}$. Upper panel: normalized deviation from steady-state unloading rate ($\hat{v}_s$ at $\hat{z} = 1$) following a pulse of solute at $\hat{z} = 0$. The pulse decays exponentially for $\hat{F} > 1$, indicating rapid transmission of the pulse throughout the sieve tube. At $\hat{F} < 1$, however, there is a long delay between when the pulse is applied and when its effects are first observed at $\hat{z} = 1$. Lower panel: the dimensionless transit time ($\hat{\tau}_t$) is a decreasing function of $\hat{F}$, approaching unity at $\hat{F} > 1$. Thus, both information and material are transported faster, in dimensionless terms, at $\hat{F} > 1$.

The rapid propagation of solute fronts present at high values of $\hat{F}$ is further illustrated by the impulse-induced temporal deviation of the solute concentration profile from steady-state (Fig. 3). At $\hat{F} = 10$, an impulse leads to a homogeneous increase in pressure and solute concentration throughout the sieve tube. The profile's decay back to steady state is exponential, following the linear unloading dynamics imposed by Eqn 4. When $\hat{F} = 0.1$, the pulse first builds locally and then propagates axially, resulting in an inhomogeneous distribution of solute and almost twice as much time to decay as in the high-$\hat{F}$ case. Only by $\hat{t} = 0.5$ does the profile's deviation approach homogeneity. The behaviour observed at $\hat{F} = 1$ shows a sieve tube at the cusp of these extremes.

Wave propagation time can be measured numerically by applying a sinusoidally varying impulse of solute influx (Eqn 8) and following the resulting waves in solute concentration. Example results for $\hat{F} = 0.1$, 1 and 10 are shown in Fig. 4 (a Huber plot, see Ferrier *et al.* 1975), all three with the loading pulses applied at a dimensionless frequency $\hat{f} = 1$. The three sieve tubes act as low-pass filters of varying strength. At high $\hat{F}$, pulse attenuation is small, and wave propagation fast. At low $\hat{F}$, however, the waves are slow (Fig. 2), longer than the period of oscillation in loading rate, such that the input signal is heavily damped. If the oscillation period is small relative to the wave propagation time,

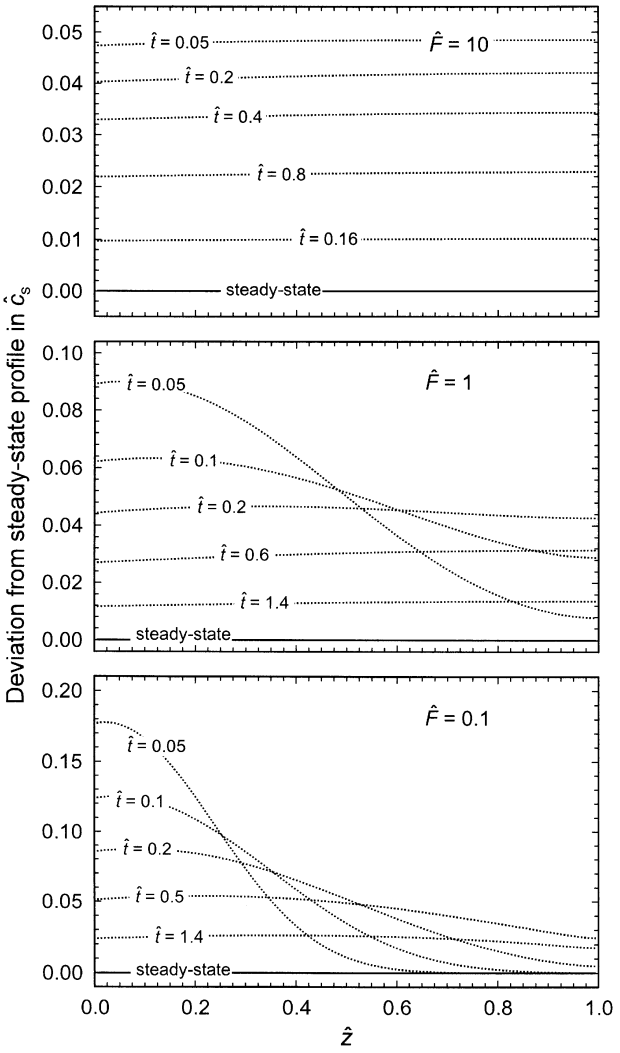

Figure 3. Deviation from the steady-state concentration profile following a pulse of solute at $\hat{z} = 0$ as a function of $\hat{F}$ (10, 1, 0.1). At $\hat{F} = 10$, solute concentration is well coupled throughout the sieve tube, but at $\hat{F} = 0.1$, there is a long delay ($\Delta\hat{t} = 0.2$) between when the solute is first applied and when it is observed at $\hat{z} = 1$. At $\hat{F} = 1$, there is a small delay, but solute is distributed evenly throughout the sieve tube by $\hat{t} = 0.2$.

then the waves become 'clipped', such that a downward swing in $\hat{c}_s$ at $\hat{z} = 1$ is brought up sooner than normal by the subsequent upward swing in solute concentration at $\hat{z} = 0$. In fact, the numerically calculated dimensionless wave propagation time ($\hat{\tau}_p$) depends on both $\hat{F}$ *and* $\hat{f}$ (Fig. 5). At high $\hat{F}$ however, variation in $\hat{\tau}_p$ closely follows Eqn 10 ($\hat{\tau}_p \approx 1/2\hat{F}$), and is $\hat{f}$-independent (for example, $\hat{\tau}_p = 0.01$ at $\hat{F} = 50$). The deviation from Eqn 10 at low $\hat{F}$ is due to the low-pass filtering behaviour of the system, which causes significant signal attenuation.

These theoretical propagation times can be compared against measurement. Huber *et al.* (1937) measured sieve sap concentrations from cut bark at various heights in individuals of *Quercus borealis*. Concentrations were found to vary diurnally, but with an increasingly large temporal phase shift with decreasing sampling height. They erroneously interpreted this phase shift as a measure of sap velocity. From those data, Ferrier *et al.* (1975) calculated a phase velocity of between 1.5 and 4.5 m h^{-1}, but, following Zimmermann (1969), argued that the actual solution velocity was 0.25 m h^{-1}. The ratio of these two velocities (solution velocity to phase velocity) is equivalent to $\hat{\tau}_p$, which here would be between 0.06 and 0.2. Huber *et al.* (1937) worked with 10-m-tall trees. Over that distance, the diurnal (24 h) dimensionless frequency would be $\hat{f} = 24\text{ h}/\tau = 24\text{ h}/(10\text{ m}/0.25\text{ m h}^{-1}) = 0.6$. Hence, sieve tubes in the trunk of *Quercus borealis* probably operate at values of $\hat{F}$ between 2.6 and 7 (found graphically from Fig. 5), and with a fairly small axial pressure drop, even over a distance of 10 m. The transit time would be about 40 h, but wave propagation could require as little as 2.6 to 8 h.

Length transects, using sieve tube scales and parameters appropriate to *R. communis* and *R. pseudoacacia*, show that solute waves are highly attenuated in long sieve tubes (10 m < L < 100 m), but that they propagate freely in shorter sieve tubes (Fig. 5). The sieve tubes of *R. communis* are highly conductive. If we assume that they are not much longer than 1.0 m, and that their sap velocity is about 1.44 m h^{-1} (see Methods), then the expected time scale τ would be about 0.7 h (i.e. 1.0 m/1.44 m h^{-1}). The transit time would be about the same, given that $\hat{F} \approx 50$ at that length. Thus, following Eqn 10, $\hat{\tau}_p$ would be about 0.01, and the wave propagation time in *R. communis* would be about 25 s. This is of the same order of magnitude as the elastic response time (Fig. 6). In other words, wave propagation in *R. communis* operates at or near the elastic limit suggested by Kallarackal & Milburn (1985).

As expected, the pressure drop scale (Π) and all the relevant time scales increase in magnitude with sieve tube length in *R. pseudoacacia*. However, some of the time scales increase faster than others. The transit time, τ_t, exceeds the system time scale, τ, at low $\hat{F}$ (see Fig. 2), and the wave propagation time, τ_p, is lower than τ at all $\hat{F}$, but especially so at high $\hat{F}$ (Fig. 6). At small L, concentration waves propagate as much as two orders of magnitude faster than the solution itself, limited only by the membrane and elastic properties of the sieve tube walls.

A sudden change in the spatial gradient in apoplastic water potential *against* the flow of sap leads to a transient drop in the rate of solute unloading at $\hat{z} = 1$ (Fig. 7). The size and duration of this response depends on $\hat{F}$, where at $\hat{F} > 1$ a negative transient is hardly perceptible, whereas at lower values of $\hat{F}$ it can become quite large.

DISCUSSION

The central finding of this work is that local perturbations in sieve tube solute concentration and pressure can be rapidly transmitted over long distances in response to any physicochemical perturbation that locally alters the water potential of the sap or apoplast (Figs 5 & 7), and especially when the sieve tube's axial pressure differential is relatively

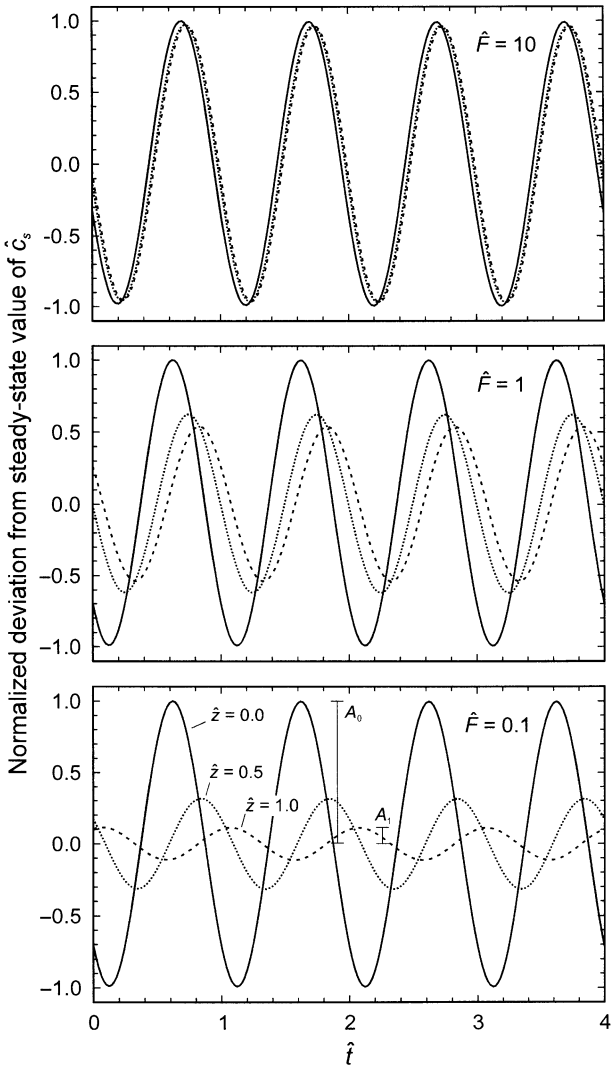

Figure 4. Huber plots of normalized variation in concentration at three points ($\hat{z}$ = 0, 0.5, and 1) along sieve tubes of $\hat{F}$ = 10, 1, and 0.1. Each sieve tube is sinusoidally forced (Eqn 8) with $\hat{d}$ = 0.01 and $\hat{f}$ = 1, and run to a quasi-steady-state (see Methods). A_0 and A_1 are the amplitudes of the concentration waves at $\hat{z}$ = 0 and 1, respectively.

small (i.e. at high $\hat{F}$). While Kallarackal & Milburn (1985) argued that the primary limitation to the movement of pressure waves was the sieve tube's elastic and membrane properties (τ_ϵ), it appears that a more important factor is $\hat{F}$, the ratio of solution osmotic pressure to the magnitude of the axial pressure drop (Fig. 6).

Sieve sap is osmotically coupled to the apoplast through a semi-permeable membrane. A local increase in concentration leads to an influx of water and locally high turgor (Fig. 8), which propagates as a wave along the length of the sieve tube (at a rate that depends predominantly on $\hat{F}$, but also on τ_ϵ at low L; Figs 5 & 6). The wave transiently raises the water potential of the sap, resulting in an efflux of water that concentrates the solute already present until water potential equilibrium is regained. This behaviour is in stark contrast to our intuition of how a 'pipe' ought to work. For instance, a fluid-filled steel pipe rapidly transmits changes in pressure, but solutes move only as fast as the bulk flow of solution will carry them. In the phloem, the two are coupled.

The freedom of movement of a pressure/concentration wave in the phloem depends solely on the phloem transport scale, $\hat{F}$. The more energy dissipated by the phloem in translocation relative to the osmotic pressure of the sap (i.e. as $\hat{F}$ decreases), the more the propagation of concentration and pressure becomes coupled to the bulk movement of the solution. That is to say, at low values of $\hat{F}$, pulses of pressure and concentration are more likely to accumulate than propagate. Sieve tubes of high $\hat{F}$ behave like high-pressure manifolds (i.e. like good household plumbing or municipal water distribution), or like low output impedance electrical circuits or high voltage power distribution lines. In each of these systems, energy is delivered at high potential with minimal differences in potential between access points, so that the entire system behaves as a single unit. No one point in the system is privileged, since changes in system state at one site are immediately distributed to all others. Although not discussed in exactly these terms by Eschrich, Evert & Young (1972), their 'volume-flow' hypothesis posits a very similar system to the one defined by a sieve tube operating at high $\hat{F}$.

It seems natural to suppose, then, that the phloem should 'design' its sieve tubes to maintain a high value of $\hat{F}$. However, to protect its sap, a sieve tube is heavily interspersed with resistive sieve plates, which the plant plugs in response to mechanical damage or herbivory. In many plants (such as *Beta vulgaris*, see Thompson & Holbrook 2003b), sieve plate resistance may comprise as much as 90% of the total axial resistance of the sieve tube; others, less so (e.g. *R. communis*). As a result, sieve tubes (especially long ones) are immediately biased toward having a large pressure drop. Perhaps it is for this reason that phloem solute concentration and turgor are kept so high; the negative effect that a moderate axial pressure drop would have on pressure/concentration wave propagation would be overcome by the much higher osmotic pressure (that is, $\hat{F}$ will increase provided Ψ_π increases faster than Π). Moreover, at higher Ψ_π the velocity required to maintain the same solute flux density will be lower, leading to a decline in the pressure drop provided there were not also a significant increase in viscosity (Lang 1978). There are other design considerations that could also be addressed relating to trade-offs between whole-axis solute flux, sieve sap velocity, sieve plate geometry, and the number of sieve tubes per axis, but they are unfortunately beyond the scope of this work.

There is considerable experimental evidence, both direct and circumstantial, that solute flux in the phloem is controlled by a pressure feedback regulatory system, though the details of such a system are not yet known (Lalonde *et al.* 2003; van Bel 2003). Phloem pressure regulation is also supported by an argument from necessity – that all plant cells must maintain a relatively constant turgor to maintain physiological function. But

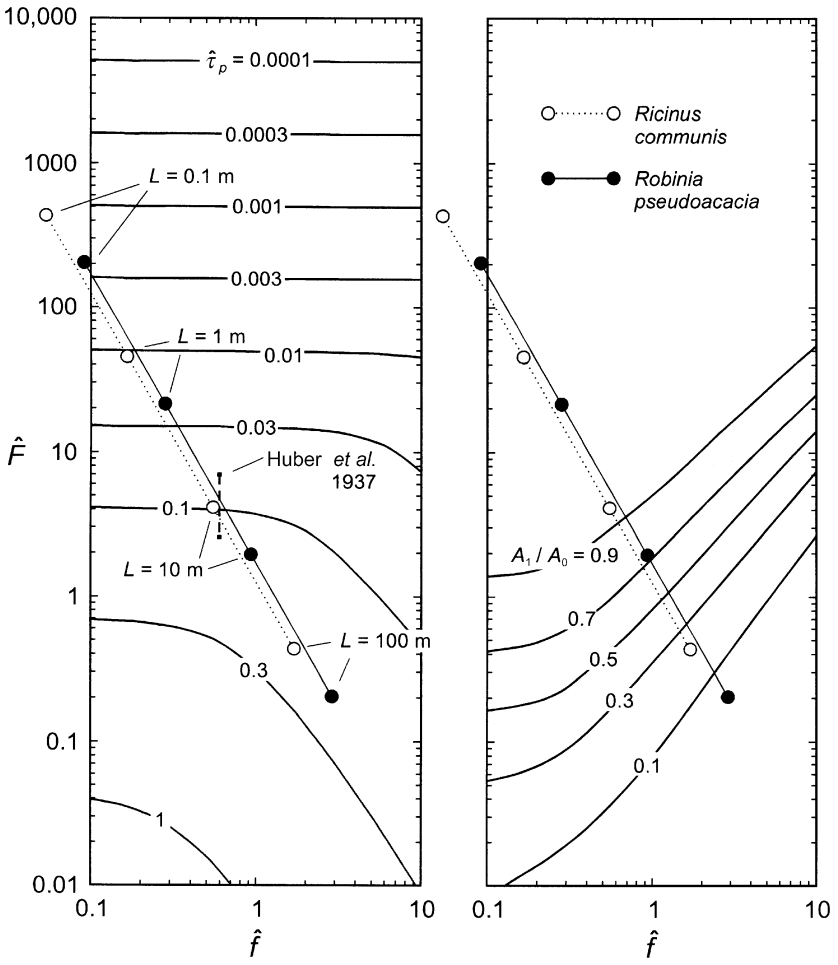

Figure 5. Dimensionless propagation time ($\hat{\tau}_p$, left panel) and amplitude attenuation (A_1/A_0, right panel; see Fig. 4) as a function of $\hat{f}$ and $\hat{F}$ (225 simulations of Eqn 2 for 25 logarithmically spaced values of $\hat{F}$ between 0.01 and 10 000 at 4 per decade, and 9 logarithmically spaced values of $\hat{f}$ between 0.1 and 10 at 4 per decade). $\hat{\tau}_p$ is the dimensionless time required for the wave peak (see Fig. 4) to go the length of the sieve tube. The dotted diagonal line corresponds to the position of *Ricinus communis* in this space as a function of sieve tube length (open circles), and the solid diagonal line corresponds to the position of *Robinia pseudoacacia* (closed circles). For both length transects, all other parameters and scales are set as described in the text, and $\hat{f}$ is a function of the length-dependent time scale, such that $\hat{f} = \tau/24$ h. The vertical, dashed line corresponds to the probable position in $\hat{F}$ $\hat{f}$-space of Huber *et al*. (1937) *Quercus borealis* trunk sieve tubes.

turgor regulation of phloem function finds support in the mechanics of phloem transport, as well. Although water potential equilibrium ensures that changes in solute concentration and pressure are locally coupled, it does *not* require that whole-sieve tube coupling exists between their *gradients* (see Fig. 7 of Thompson & Holbrook 2003b). The definition of water potential equilibrium ($\psi_o = p - \Re T c_s$) includes a term for apoplastic water potential, making the concentration profile as sensitive to the apoplastic water potential profile as it is to the pressure gradient:

$$\Re T \frac{dc_s}{dz} = \frac{dp}{dz} - \frac{d\psi_o}{dz} \quad (13)$$

Traditionally (see Hocking 1980), we think of $\Re T(dc_s/dz)$ as being negative (i.e. concentration drops with z). This is guaranteed to be true if phloem translocation is in the opposite direction of xylem sap flow, where $d\psi_o/dz$ is positive. Yet, precisely *because* there is water potential equilibrium, the larger $d\psi_o/dz$ becomes, the more the concentration and pressure gradients decouple (Fisher 1978). Indeed, were $d\psi_o/dz$ to become negative and of sufficiently high magnitude (i.e. phloem and xylem transport in the same direction), then the pressure and solute potential gradients could have opposite signs (see Wolswinkel 1992): phloem translocation against a concentration gradient!

For this reason, concentration cannot be a good feedback control variable. A better candidate would be turgor, which meaningfully reflects the physiological state of the system while avoiding the transmission of spurious signals. The magnitude of the pressure drop is ultimately free from the effects of changing apoplastic water potential gradients, depending as it does solely on the flow velocity, the viscosity, and the geometry and length of the sieve tube. If the phloem transport scale is large (which seems to be the case based on the limited data available, see Thompson & Holbrook 2003b), then the absolute magnitude of the pressure drop will be relatively insensitive to changes in flow rate (which varies less than a factor of 2 or 3, anyway, see Peuke *et al*. 2001), allowing turgor to be nearly the same everywhere in the system. Turgor would be highly sensitive to local, if transient, changes in apoplastic water potential or osmotic pressure, but with a global effect.

Pressure-regulated sieve tube transport (or *osmoregulatory flow*, Thompson & Holbrook 2003b) will work best only at high $\hat{F}$ (just as plumbing works best when pressure

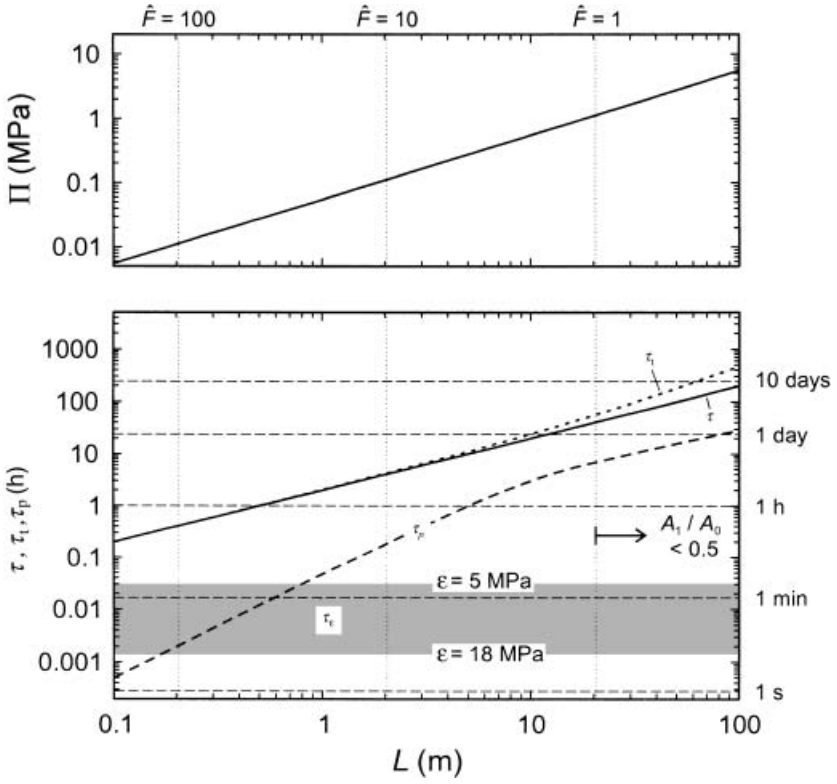

Figure 6. Pressure and temporal behaviour of a *Robinia pseudoacacia* sieve tube (same as in Fig. 5) as a function of L, using scale parameter values as described in the text (see Methods). Upper panel: the pressure scale (Π, or axial pressure drop) increases linearly with L (Eqn 6, Table 1), and becomes large relative to the osmotic potential of the sap (i.e. $\hat{F} \leq 1$) at $L > 20$ m. Lower panel: the system time scale (τ), transit time (τ_t), and wave propagation time (τ_p) all increase with L; however, τ_t increases faster than τ at low $\hat{F}$ (see Fig. 2), and the wave propagation time is always lower than the material transit time. The grey band shows the potential range of τ_ε, for ε between 5 and 18 MPa, and assuming $L_p = 5 \times 10^{-8}$ m s^{-1} MPa^{-1} and $\Psi_\pi = 2.0$ MPa. The vertical dotted lines indicate the values of $\hat{F}$, and the right-facing arrow shows where amplitude attenuation falls below $A_1/A_0 = 0.5$.

differentials are small), so that *all* sieve element/companion cell (SE/CC) complexes can be 'programmed' to respond to changes in turgor in the same or nearly the same way. Over long distances, as pressure differentials increase in magnitude, this may not be possible. If a large pressure differential has to be maintained by the sieve tube (Aloni, Wyse & Griffith 1986; Minchin & Thorpe 1987; van Bel & Knoblauch 2000; Patrick *et al*. 2001; Ayre, Keller & Turgeon 2003; van Bel 2003), then it would be necessary to 'program' the different SE/CC complexes to set-point turgor pressures that are position- and flow-rate-dependent, and to 're-program' those set-points whenever flow rate or plant architecture changed. For the decentralized plant, this could be difficult. But at high $\hat{F}$, any part of the sieve tube (whether in the collection, transport, or release phloem) could maintain turgor on behalf of the whole, using whatever solutes are available, including sucrose, sugars of the raffinose series, or inorganic and organic ions, such as potassium and malate (Lang 1983). Moreover, there is room to believe that plants might artificially raise $\hat{F}$ by decreasing the effective length (L) of transport throughout the use of apoplastic solute relays (Lang 1979; Thompson & Holbrook 2003b).

Plants lack a nervous system, and phloem translocation control must rely on locally available signals that hopefully represent the needs of tissues much further away. Individual plant cells (no bigger than a few hundred microns) can quickly deliver changes in concentration by diffusion alone. By other means, sieve tubes do the same, behaving like 'neurons' to transmit information from one part of a plant to another with little material transfer. A small axial pressure differential allows the sieve tube to transmit this information quickly and to employ changes in pressure as a means of regulating global sieve tube function.

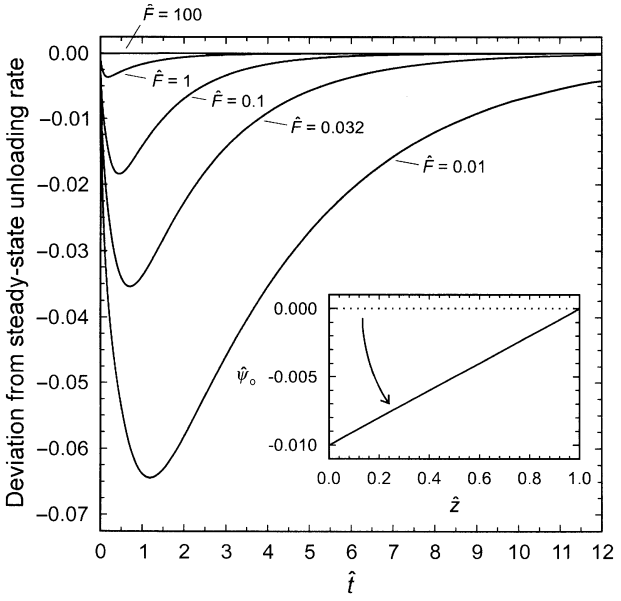

Figure 7. The deviation and recovery from the steady-state unloading rate, as a function of $\hat{F}$, after imposing an opposing gradient in apoplastic water potential ($\partial\hat{\psi}_o/\partial\hat{z}$) of magnitude 0.01 (Eqn 12).

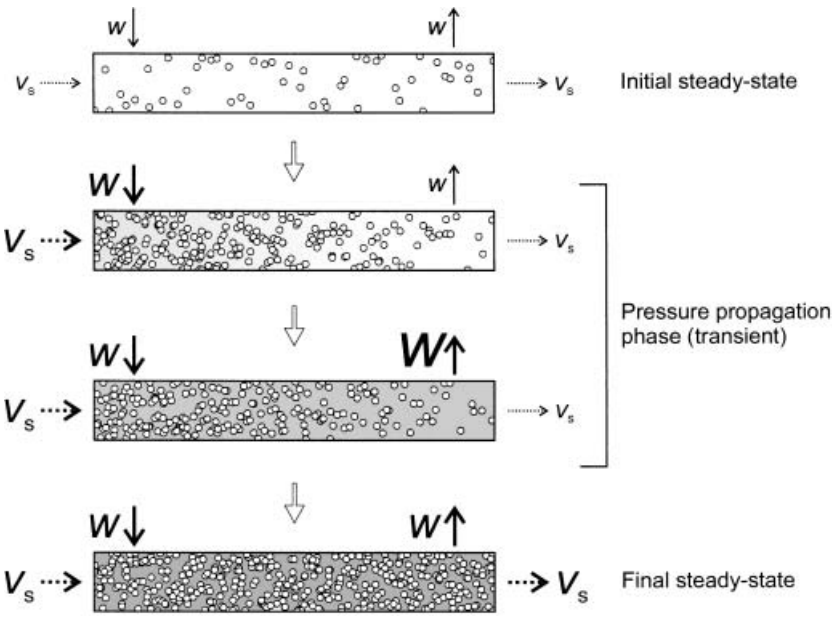

Figure 8. The propagation of pressure/concentration waves. At steady-state, solute ($\hat{v}_s$) and water flux (w) into the sieve tube equal solute and water flux out. The size of these symbols and their associated arrows denote the magnitude of each flux. The concentration of open circles is proportional to concentration, and the degree of shading in the background is proportional to pressure. For clarity's sake, we show a sieve tube with a large value of $\hat{F}$ and with no external gradient in apoplastic water potential (such that there is no distinguishable drop in concentration with length). First panel: pressure and solute concentration are initially low. Second panel: solute loading in the collection phloem increases, locally raising concentration, membrane water influx, and pressure. Third panel: this increase in pressure is rapidly propagated the length of the sieve tube, transiently raising the sap water potential relative to the apoplast and the efflux of water near the release phloem. Final panel: the terminal efflux of water concentrates the solutes, raising the solute concentration until the sieve sap is in local water potential equilibrium. The propagation velocity depends on its ability to transmit pressure ($\hat{F}$-dependent) and how fast the sieve tube can locally come to water potential equilibrium (ε, L_p, and SA:V-dependent; see Eqn 11).

ACKNOWLEDGMENTS

We thank Howard A. Stone and Maciej A. Zwieniecki for insightful discussions, and Michael J. Burns for help in interpreting the frequency response of impulses applied to dynamic systems. We also thank one anonymous reviewer, and Sanna Sevanto for considerable encouragement. This work is supported by a grant from the Andrew W. Mellon Foundation to Harvard University.

REFERENCES

Aloni B., Wyse R.E. & Griffith S. (1986) Sucrose transport and phloem unloading in stem of *Vicia faba*: possible involvement of a sucrose carrier and osmotic regulation. *Plant Physiology* **81,** 482–486.

Ayre B.G., Keller F. & Turgeon R. (2003) Symplastic continuity between companion cells and the translocation stream: long-distance transport is controlled by retention and retrieval mechanisms in the phloem. *Plant Physiology* **131,** 1518–1528.

van Bel A.J.E. (2003) The phloem, a miracle of ingenuity. *Plant, Cell and Environment* **26,** 125–149.

van Bel A.J.E. & Knoblauch M. (2000) Sieve element and companion cell: the story of the comatose patient and the hyperactive nurse. *Australian Journal of Plant Physiology* **27,** 477–487.

Berg H.C. (1993) *Random Walks in Biology*. Princeton University Press, Princeton, NJ, USA.

Dainty J. (1976) Water relations in plant cells. In *Encyclopedia of Plant Physiology*, Vol. 2 *Part A* (eds U. Lüttge & M. Pitman), pp. 12–35. Springer-Verlag, New York, USA.

Eschrich W., Evert R.F. & Young J.H. (1972) Solution flow in tubular semipermeable membranes. *Planta* **107,** 279–300.

Ferrier J.M. (1976) An approximate analytic equation for sugar concentration waves in Münch phloem translocation systems. *Canadian Journal of Botany* **54,** 2130–2132.

Ferrier J.M., Tyree M.T. & Christy A.L. (1975) The theoretical time-dependent behavior of a Münch pressure-flow system: the effect of sinusoidal time variation in sucrose loading and water potential. *Canadian Journal of Botany* **53,** 1120–1127.

Fisher D.B. (1978) An evaluation of the Münch hypothesis for phloem transport in soybean. *Planta* **139,** 25–28.

Goeschl J.D. & Magnuson C.E. (1986) Physiological implications of the Münch-Horwitz theory of phloem transport: effect of loading rates. *Plant, Cell and Environment* **9,** 95–102.

Hocking P.J. (1980) The composition of phloem exudate and xylem sap from tree tobacco (*Nicotiana glauca* Grah.). *Annals of Botany* **45,** 633–643.

Huber B., Schmidt E. & Jahnel H. (1937) Untersuchungen über den Assimilationsstrom der Bäume I. *Tharandter Forstliches Jahrbuch* **88,** 1017–1049.

Kallarackal J. & Milburn J.A. (1985) Phloem sap exudation in *Ricinus communis*: elastic responses and anatomical implications. *Plant, Cell and Environment* **8,** 239–245.

Lalonde S., Tegeder M., Throne-Holst M., Frommer W.B. & Patrick J.W. (2003) Phloem loading and unloading of sugars and amino acids. *Plant, Cell and Environment* **26,** 37–56.

Lang A. (1978) A model of mass flow in the phloem. *Australian Journal of Plant Physiology* **5,** 535–546.

Lang A. (1979) A relay mechanism for phloem translocation. *Annals of Botany* **44,** 141–145.

Lang A. (1983) Turgor-regulated translocation. *Plant, Cell and Environment* **6,** 683–689.

Lee D.R. (1981) Synchronous pressure-potential changes in the phloem of *Fraxinus americana* L. *Planta* **151,** 304–308.

Mason T.G. & Maskell E.J. (1928a) Studies on the transport of carbohydrates in the cotton plant. I. A study of diurnal variation in the carbohydrates of leaf, bark and wood, and of the effects of ringing. *Annals of Botany* **42,** 189–253.

Mason T.G. & Maskell E.J. (1928b) Studies on the transport of carbohydrates in the cotton plant. II. The factors determining the rate and the direction of movement of sugars. *Annals of Botany* **42,** 571–636.

Minchin P.E.H. & Thorpe M.R. (1987) Measurement of unloading and reloading of photo-assimilate within the stem of bean. *Journal of Experimental Botany* **38,** 211–220.

Minchin P.E.H., Thorpe M.R. & Farrar J.F. (1993) A simple mechanistic model of phloem transport which explains sink priority. *Journal of Experimental Botany* **44,** 947–955.

Moorby J., Troughton J.H. & Currie B.G. (1974) Investigations of carbon transport in plants. II. The effects of light and darkness and sink activity on translocation. *Journal of Experimental Botany* **25,** 937–944.

Patrick J.W., Zhang W., Tyerman S.D., Offler C.E. & Walker N.A. (2001) Role of membrane transport in phloem translocation of assimilates and water. *Australian Journal of Plant Physiology* **28,** 695–707.

Peuke A.D., Rokitta M., Zimmermann U., Schreiber L. & Haase A. (2001) Simultaneous measurement of water flow velocity and solute transport in xylem and phloem of adult plants of *Ricinus communis* over a daily time course by nuclear magnetic resonance spectrometry. *Plant, Cell and Environment* **24,** 491–503.

Thompson M.V. & Holbrook N.M. (2003a) Application of a single-solute non-steady-state phloem model to the study of long-distance assimilate transport. *Journal of Theoretical Biology* **220,** 419–455.

Thompson M.V. & Holbrook N.M. (2003b) Scaling phloem transport: water potential equilibrium and osmoregulatory flow. *Plant, Cell and Environment* **26,** 1561–1577.

Wolswinkel P. (1992) Transport of nutrients into developing seeds: a review of physiological mechanisms. *Seed Science Research* **2,** 59–73.

Zimmermann M.H. (1969) Translocation velocity and specific mass transfer in the sieve tubes of *Fraxinus americana* L. *Planta* **84,** 272–278.

Received 30 June 2003; received in revised form 14 October 2003; accepted for publication 16 October 2003